

## Hydrostatic pressure control of the magnetostructural phase transition in $\text{Gd}_5\text{Si}_2\text{Ge}_2$ single crystals

C. Magen,<sup>1</sup> L. Morellon,<sup>1,\*</sup> P. A. Algarabel,<sup>1</sup> M. R. Ibarra,<sup>1</sup> Z. Arnold,<sup>2</sup> J. Kamarad,<sup>2</sup> T. A. Lograsso,<sup>3</sup> D. L. Schlagel,<sup>3</sup> V. K. Pecharsky,<sup>3,4</sup> A. O. Tsokol,<sup>3</sup> and K. A. Gschneidner, Jr.<sup>3,4</sup>

<sup>1</sup>*Departamento de Física de la Materia Condensada and Instituto de Ciencia de Materiales de Aragón, Universidad de Zaragoza and Consejo Superior de Investigaciones Científicas, 50009 Zaragoza, Spain*

<sup>2</sup>*Institute of Physics AS CR, Na Slovance 2, 182 21 Prague 8, Czech Republic*

<sup>3</sup>*Materials and Engineering Physics Program, Ames Laboratory, Iowa State University, Ames, Iowa 50011-3020, USA*

<sup>4</sup>*Department of Materials Science and Engineering, Iowa State University, Ames, Iowa, 50011-2300, USA*

(Received 24 January 2005; published 8 July 2005)

Magnetic and structural properties of single crystalline  $\text{Gd}_5\text{Si}_2\text{Ge}_2$  under hydrostatic pressure have been characterized by using magnetization, linear thermal expansion, and compressibility measurements. A strong dependence of Curie temperature on pressure,  $dT_C/dP = +4.8$  K/kbar, is observed in contrast with the smaller values of about 3 K/kbar found in polycrystalline specimens. This difference reflects the role the microstructure may play in pressure-induced magnetic-crystallographic phase changes, likely related to stress relaxation at the grain boundaries, domain pinning and/or nucleation of defects. The pressure dependence of the critical magnetic field,  $d(dH_C/dT)/dP$ , drops at the rate  $-0.122(5)$  kOe/K kbar, which points to an enhancement of the magnetoelastic coupling with pressure. The latter affects the magnetocaloric behavior of the material at the rate  $d(\Delta S_M)/dP \cong 1.8$  J/kg K kbar. The linear thermal expansion confirms the strongly anisotropic change of the lattice parameters through the orthorhombic to monoclinic crystallographic transformation with  $\Delta a/a = +0.94\%$ ,  $\Delta b/b = -0.13\%$ , and  $\Delta c/c = -0.22\%$ . The structural transition temperature varies with pressure synchronously with the Curie temperature, and the size and shape of the strain anomalies remain nearly unaffected by the hydrostatic pressure, indicating, respectively, that the structural and magnetic transformations remain coupled, and the anisotropic behavior of the lattice is preserved as pressure increases. The room temperature linear compressibility data show that the magnetostructural transformation can be triggered isothermally at  $\sim 6$  kbar and that the compressibility is anisotropic.

DOI: [10.1103/PhysRevB.72.024416](https://doi.org/10.1103/PhysRevB.72.024416)

PACS number(s): 75.30.Kz, 62.50.+p, 75.50.Cc

### I. INTRODUCTION

The  $\text{Gd}_5\text{Si}_x\text{Ge}_{4-x}$  family of rare-earth intermetallic compounds was reported by Holtzberg *et al.* nearly 40 years ago.<sup>1</sup> However, these materials received little attention before 1997, when the giant magnetocaloric effect (GMCE) was discovered in  $\text{Gd}_5\text{Si}_2\text{Ge}_2$  by Pecharsky and Gschneidner.<sup>2</sup> The largest near room temperature magnetocaloric effect observed to that date in the elemental Gd was nearly doubled. Following this finding, a number of potential near ambient applications have emerged in the field of magnetic refrigeration, which is an environmentally friendly technology due to the absence of ozone depleting and greenhouse chemicals, and which is based on high efficiency electronic processes to produce temperature lift when compared to the conventional vapor-compression refrigeration technique.<sup>3</sup> A broad interest in the  $\text{Gd}_5\text{Si}_x\text{Ge}_{4-x}$  materials was also developed in order to uncover the physical fundamentals governing their potent magnetocaloric effect.<sup>4,5</sup>

The physics of the  $\text{Gd}_5\text{Si}_x\text{Ge}_{4-x}$  system is intimately related to the varying crystal structures of its members. A total of 36 atoms per unit cell are assembled into two-dimensional layers, i.e., the *slabs* whose spatial arrangement is determined by the number of partially covalent Si/Ge-Si/Ge bonds (0, 2, or 4 covalently bonded pairs of atoms per unit cell) between neighboring slabs. A change in the number of the interslab  $\text{Si}_2$  ( $\text{Ge}_2$  or SiGe) pairs drastically modifies

crystallography,<sup>6-8</sup> electronic structure,<sup>9-12</sup> and magnetic interactions.<sup>13-16</sup> Whereas the main intralayer magnetic interactions can be treated by the Rudermann-Kittel-Kasuya-Yosida (RKKY) indirect  $4f-4f$  exchange, commonly accepted as the main magnetic contribution in  $4f$  intermetallics, the formation of covalentlike interslab bonds is capable of enhancing the interlayer coupling by means of a superexchange-type interaction mediated via Si/Ge-Si/Ge bonds, thus allowing the existence of different magnetic states.<sup>17,18</sup> As a matter of fact, a coupled magnetostructural phase transition occurs near 270 K in  $\text{Gd}_5\text{Si}_2\text{Ge}_2$  where the high-temperature paramagnetic (PM) phase adopts the monoclinic (*M*) structure with half of the interslab bonds broken and the low-temperature ferromagnetic (FM) phase realizes the orthorhombic [*O*(I)] state with all of the Si/Ge-Si/Ge pairs reformed.<sup>18</sup> The coexistence of the crystallographic transformation with the FM ordering gives rise to an additional source of the magnetic field-induced isothermal entropy change, consequently providing the explanation of the GMCE.<sup>19</sup> Thus, this transformation can be reversibly induced by changing temperature and/or magnetic field, which is at the origin of the rich and complex phenomenology that has been described in previous publications.<sup>1,5,13,17,20-27</sup>

Hydrostatic pressure is yet another intensive thermodynamic variable that can affect either or both the magnetic and structural properties of materials, and it is currently becoming

ing an important additional external parameter of interest in order to more completely comprehend the microscopic processes taking place in the 5:4 materials. An earlier investigation of several alloys from the  $\text{Gd}_5\text{Si}_x\text{Ge}_{4-x}$  series with  $x=3.2, 1.8,$  and  $0.4$  allowed us to provide a clear evidence that the effect of pressure is that of reinforcing the interslab exchange interactions via the reduction of the cell volume, thus stabilizing the  $O(\text{I})$  phase, and therefore increasing the transition temperature of the transformation.<sup>28</sup> This effect becomes especially significant at the magnetostructural transformation in the  $0 < x < \sim 2$  composition range. For example,  $dT_C/dP = +3.0$  K/kbar when  $x=1.8$ , i.e., where there is a large phase volume change associated with the transformation, yet the rates of change of the critical temperatures are about an order of magnitude smaller for the purely magnetic transitions,<sup>29</sup> i.e.,  $dT_C/dP = +0.3$  K/kbar when  $x=3.2$ , or  $dT_N/dP = +0.7$  K/kbar when  $x=0.4$ ; in both cases, there are no associated structural changes. Similarly, large differences in  $dT_C/dP$  depending on the nature of the transition were also observed in  $\text{Tb}_5\text{Si}_2\text{Ge}_2$ , where the structural and magnetic transformations at atmospheric pressure are separated by  $\sim 10$  K. In this compound, hydrostatic pressure was shown to be a tool facilitating a recoupling of both the crystallographic and magnetic transitions resulting in a spectacular enhancement of the MCE in this compound,<sup>30,31</sup> opening up a route for improving the magnetic refrigerant properties of the material. More intriguing effects were found in  $\text{Gd}_5\text{Ge}_4$ , which at ambient pressure preserves the antiferromagnetic (AFM)  $O(\text{II})$  state at low temperatures—the only exception in the  $\text{Gd}_5\text{Si}_x\text{Ge}_{4-x}$  series where the ground state is always FM  $O(\text{I})$ .<sup>19,21</sup> In this system, the application of hydrostatic pressure favors, as expected from thermodynamics, the formation of the low volume FM  $O(\text{I})$  phase, initially giving rise to an inhomogeneous, spatially segregated state composed of AFM  $O(\text{II})$  and FM  $O(\text{I})$  phases. Eventually, at high enough pressure, i.e., 10 K bar, a thermodynamically stable FM  $O(\text{I})$  state with  $T_C \cong 57$  K sets in the whole sample volume.<sup>32</sup>

All of the studies mentioned above were performed on polycrystalline specimens where some aspects of the physical behavior of these systems may be masked or averaged out, mainly those associated with anisotropic properties.<sup>33,34</sup> Furthermore, the possibility of isothermally inducing the magnetostructural transformation in zero field by means of hydrostatic pressure also seems plausible, yet no experimental evidence has been provided. Single crystal specimens are most suitable in order to carry out this type of a study. The aim of the present work is to investigate the magnetic and structural properties of single crystalline  $\text{Gd}_5\text{Si}_2\text{Ge}_2$  under hydrostatic pressure. The possibility of inducing the magnetostructural transformation by applying hydrostatic pressure is explored by means of magnetization, LTE, and isothermal compressibility experiments.

## II. EXPERIMENT

Single crystals of  $\text{Gd}_5\text{Si}_2\text{Ge}_2$  were prepared by the Bridgman method.<sup>35</sup> Appropriate quantities of gadolinium (99.996 wt %), silicon (99.9999 wt %), and germanium (99.999

wt %) were arc melted under a high purity argon atmosphere. The buttons were then remelted to ensure compositional homogeneity throughout the ingot, and the alloy was drop cast into a copper chill mold. The ingot was sealed in a tungsten Bridgman crucible, which has been electron-beam welded shut, for crystal growth and heated in a tungsten mesh resistance furnace under a pressure of  $8.8 \times 10^{-5}$  Pa up to 1000 °C and held at this temperature for one hour to degas both the crucible and the charge. The chamber was then backfilled to a pressure of  $3.4 \times 10^4$  Pa with high-purity argon. This overpressurization was done in order to equalize the pressure inside and outside of the crucible at the final temperature. The ingot was then heated to 2000 °C and held at this temperature for 1 h to allow thorough mixing before withdrawing the sample from the heat zone at a rate of 4 mm/h. The as-grown crystal was oriented by backreflection Laue and the crystallographic directions assigned using x-ray diffraction two-theta scans of the single crystal. Two samples were cut by spark erosion with two parallel planes perpendicular to  $a$  and  $b$  axis, respectively, and the faces were polished using standard metallographic techniques.

Magnetic measurements were performed in a commercial (Quantum Design) superconducting quantum interference device (SQUID) magnetometer in applied magnetic fields up to 50 kOe in the temperature range 5–300 K. Pressure experiments were carried out using a miniature CuBe pressure cell. The pressure was determined at low temperatures measuring the pressure dependence of the superconducting transition temperature of a lead sensor located inside the cell. An increase of pressure in the clamped cell with increasing temperature was taken into account. The values of pressure given in the figures correspond to actual pressures at the listed temperature intervals.

Linear thermal expansion (LTE) in the temperature range 5–300 K and isothermal compressibility were measured using the strain-gauge technique in a conventional close-cycle cryostat. Hydrostatic pressures up to 9 kbar were applied by using a standard CuBe piston-cylinder cell and in this case, the pressure values were determined over the entire temperature range by using a calibrated Manganin sensor.

## III. RESULTS

The zero pressure (out-of-pressure-cell) magnetic properties of the single crystals were measured prior to the pressure studies in order to further check the quality and the behavior of the sample. Figure 1(a) illustrates the temperature dependencies of the low-field (100 Oe) magnetization in the temperature range 5–350 K along the three crystallographic axes, showing sharp anomalies at the transition temperature  $T_C = 267.3(5)$  K upon heating. A smooth increase of the magnetization along the  $a$  axis is found on cooling, which is likely associated with a spin reorientation process. These results clearly show that the  $a$  axis is the easy magnetization axis at  $T=5$  K and  $c$  direction appears to be the hard magnetization axis. This is consistent with the behavior of magnetization isotherms measured with the magnetic field applied along the different crystallographic axes at 5 K, which are plotted in Fig. 1(b). A saturation magnetization value of

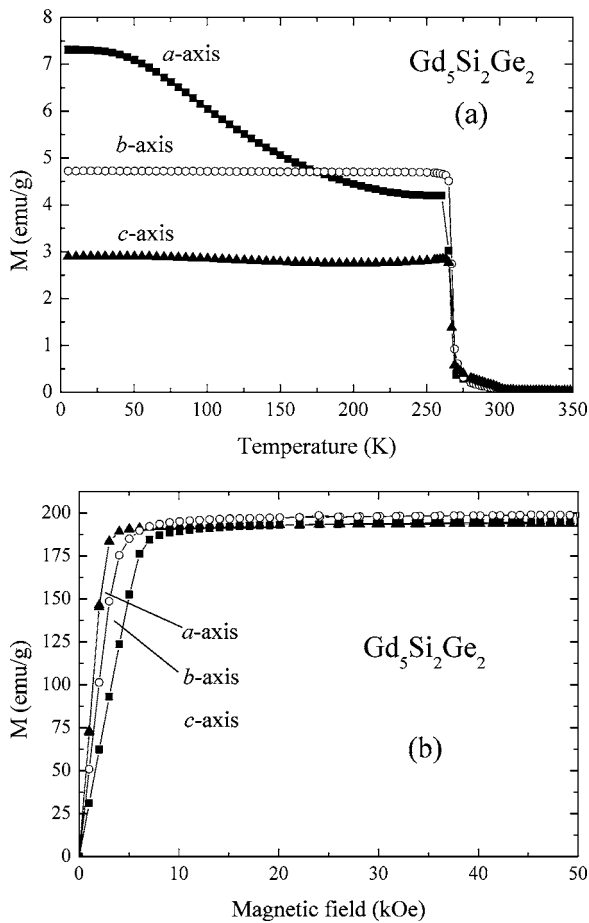


FIG. 1. Zero-pressure magnetic characterization of the  $Gd_5Si_2Ge_2$  single crystal along the three crystallographic axes: (a) Magnetization as a function of temperature in a magnetic field of  $H=100$  Oe. (b) Field dependence of magnetization at  $T=5$  K.

$M_S=197$  emu/g is obtained in a magnetic field of 50 kOe, yielding a magnetic moment of  $6.98 \mu_B$  per Gd atom, which is in excellent agreement with the theoretical  $gJ$  value of  $7 \mu_B$  for the  $Gd^{3+}$  ion.

Isofield magnetization experiments under hydrostatic pressure were performed with the magnetic field vector applied along the  $a$ -axis of a crystal in a SQUID magnetometer. Temperature dependencies of the low-field magnetization at different pressure values are displayed in Fig. 2. It is easy to see that the magnetic transformation moves towards higher temperature values at a rate of  $dT_C/dP=+4.6(2)$  K/kbar on cooling and  $+4.9(4)$  K/kbar on heating; the difference in the rates of change of Curie temperature is statistically insignificant. These values are nearly 60% higher than  $+3.0$  K/kbar reported for polycrystalline specimens of  $Gd_5Si_{1.8}Ge_{2.2}$ ,<sup>28</sup> which exhibit a magnetostructural transition identical to that of the  $Gd_5Si_2Ge_2$  material used in this study. The transition retains its first-order character within the pressure range studied, as can be deduced from the hysteretic behavior ( $\sim 3$ – $5$  K) and from the little variation in the sharpness of the anomaly. Sets of magnetization isotherms as functions of magnetic field at fixed pressures of 0, 3.7, and 5.2 kbar are shown in Figs. 3(a)–3(c), respectively. The critical field ( $H_C$ ) at a given temperature rapidly decreases with increasing

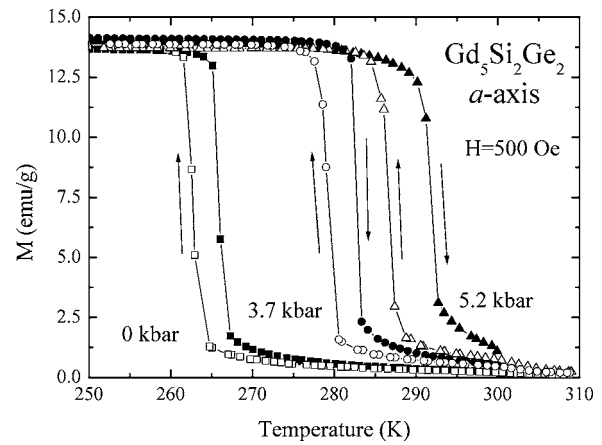


FIG. 2. Pressure dependence of the magnetization in the proximity of the magnetostructural transition measured with a 500 Oe magnetic field applied along the  $a$ -direction. Open symbols are used for the cooling curves and filled symbols for the heating runs. The different curves are labelled with the corresponding pressure values.

pressure, as expected due to the pressure-induced isofield shift of the transition temperature. Furthermore, the dependence of the critical field on temperature is notably affected by increasing pressure. This is clearly seen in Fig. 4, where  $H_C$  has been represented as a function of temperature at selected pressures. A linear thermal dependence of  $H_C$  is also noticeable, resulting in  $dH_C/dT$  values of  $+1.69(1)$  kOe/K at 0 kbar,  $+1.22(3)$  kOe/K at 3.7 kbar, and  $+1.06(3)$  kOe/K at 5.2 kbar. The zero pressure value of  $dH_C/dT$  agrees well with the previous results published by Tang *et al.*<sup>34</sup> (i.e.,  $dH_C/dT=+1.8$  kOe/K). The slope  $dH_C/dT$  decreases linearly with increasing pressure at the rate  $d(dH_C/dT)/dP=-0.122(5)$  kOe/K kbar, which reflects the strengthening of the magnetoelastic coupling upon increasing the applied hydrostatic pressure. This result is consistent with the evolution of  $dH_C/dT$  as a function of composition ( $x$ ) throughout the  $Gd_5Si_xGe_{4-x}$  series reported by Casanova *et al.*<sup>36</sup>

As one might expect, the enhancement of the magnetoelastic coupling should result in a smaller value of the magnetocaloric effect.<sup>36,37</sup> We have confirmed this point by estimating the isothermal change in entropy  $\Delta S_M$  from the measurements shown in Fig. 3 by both numerically integrating the Maxwell relation  $dS_M=(dM/dT)_H dH$  and by using the Clausius–Clapeyron equation  $\Delta S_M=(dH_C/dT)\Delta M$ . A reduction of  $d(\Delta S_M)/dP$  at a rate of  $1.8$  J/kg K kbar has been obtained. This particular feature could be of importance when considering potential practical applications of these alloys as magnetic refrigerant materials, although high pressures that are required to noticeably change the magnetocaloric effect are several orders of magnitude greater than pressures exerted on the magnetocaloric bed by a heat transfer fluid.<sup>38</sup>

LTE and compressibility measurements provide additional and valuable information about the magnetostructural transformation under hydrostatic pressure. As observed in Fig. 5, the  $O(I) \rightarrow M$  structural change, accompanying the magnetic disordering, is clearly seen at  $T_C=265.8(3)$  K on heating. A small difference of  $\sim 1.5$  K in the transition temperature

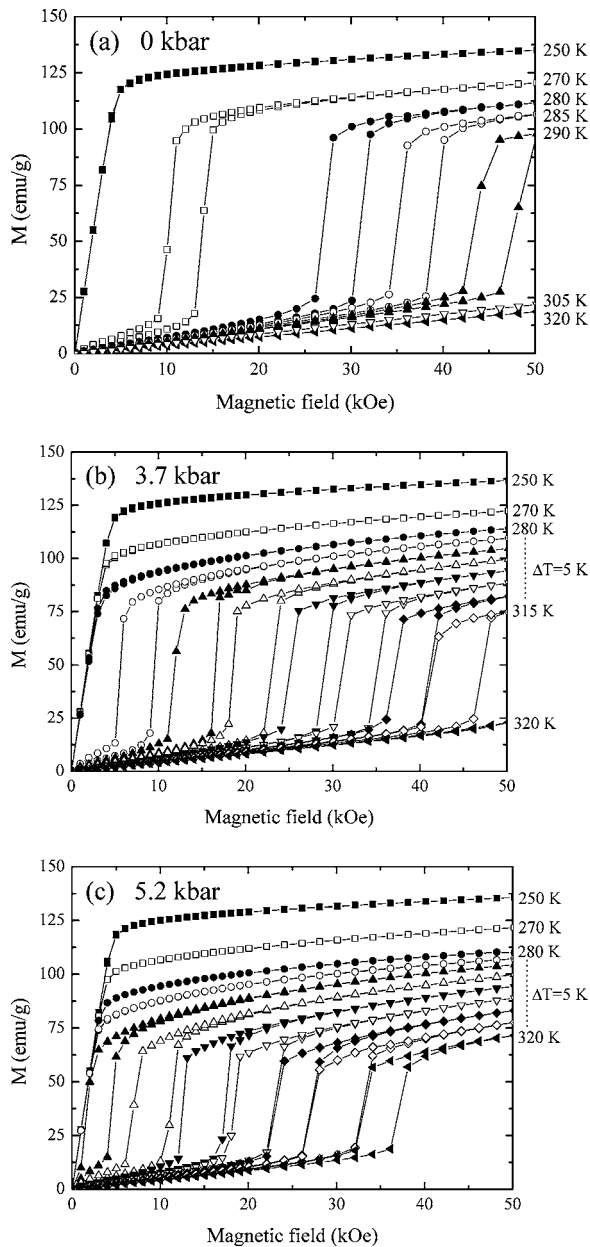


FIG. 3. Magnetization isotherms measured in the vicinity of the magnetostructural transformation with the magnetic field applied along the  $a$ -axis at different pressures: (a)  $P=0$ , (b) 3.7, and (c) 5.2 kbar. The pressure values are real pressures at  $T_C=267.3$  K. The isotherms were measured when the sample was heated from the FM state to the temperature indicated on the plots.

compared with  $T_C=267.3$  K obtained from the low-field magnetization measurements may be associated with a small temperature gradient existing between the sample and temperature sensor, which are a few centimeters apart in a close cycle refrigerator used in the LTE experiments. The changes in length at the transformation along different crystallographic directions are anisotropic,  $\Delta a/a=+0.94\%$ ,  $\Delta b/b=-0.13\%$ , and  $\Delta c/c=-0.22\%$ , the overall volume change is  $\Delta V/V=+0.6\%$ . This is in reasonable agreement with the x-ray powder diffraction studies,<sup>20,39</sup> single-crystal x-ray diffraction,<sup>7</sup> and thermal expansion data<sup>33</sup> reported for sev-

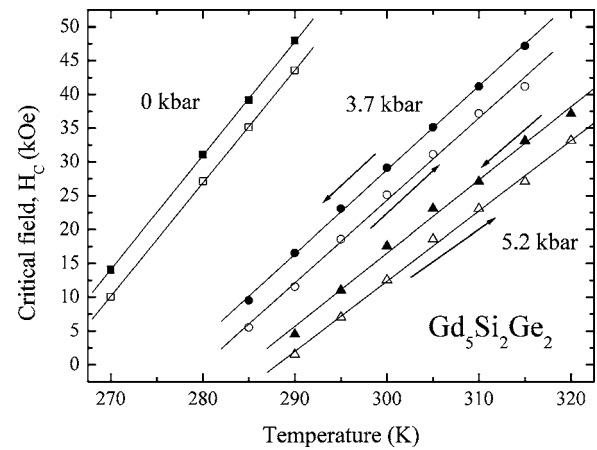


FIG. 4. Pressure dependence of the critical field  $H_C$  as a function of temperature determined from the different sets of magnetization isotherms at the three studied pressure values with the magnetic field applied along the  $a$  axis. Open symbols represent values obtained on increasing magnetic fields and full symbols are used for decreasing fields.

eral  $Gd_5Si_xGe_{4-x}$  materials with stoichiometry varying near  $x=2$ . We have also determined the thermal expansion coefficients along each crystallographic axis,  $\alpha_X=(dX/dT)/X$  from the data in Fig. 5. The obtained values at 200 K, i.e., in the  $O(I)$  structure, are  $\alpha_a=5.0 \times 10^{-6} \text{ K}^{-1}$ ,  $\alpha_b=10.4 \times 10^{-6} \text{ K}^{-1}$ , and  $\alpha_c=17.8 \times 10^{-6} \text{ K}^{-1}$ . A general trend  $\alpha_a < \alpha_b$  and  $\alpha_a < \alpha_c$  is observed, i.e., the LTE coefficient is the smallest parallel to the  $a$  axis along which the slabs slide during the structural change. These values and the trends are in good agreement with those extracted from the thermal expansion studies of single crystal of  $Gd_5Si_{1.72}Ge_{2.28}$  reported by Nazih *et al.*<sup>33</sup> and obtained from x-ray diffraction experiments of the  $Gd_5Ge_4$  alloy with the  $O(II)$  structure.<sup>40</sup>

Figure 6 illustrates the pressure dependence of the LTE along the different crystallographic axes on heating. In all cases, the anomalies are shifted to higher temperatures at a rate of  $+4.7(2) \text{ K/kbar}$ , which nearly ideally agrees with the magnetic measurements, therefore, confirming that both

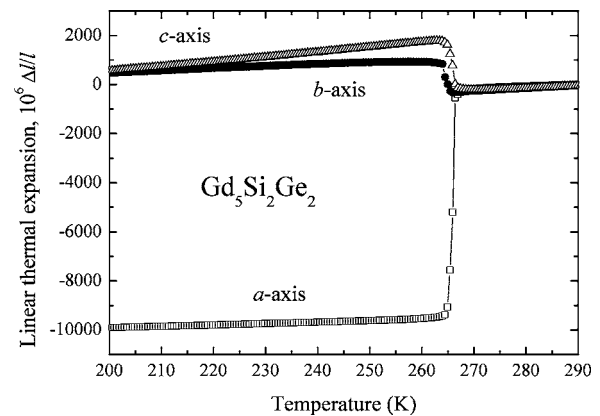


FIG. 5. LTE defined as  $\Delta l/l=l(T)/l(290 \text{ K})-1$ , where  $l=a, b$ , and  $c$  lattice parameters, in the  $Gd_5Si_2Ge_2$  single crystal. The experiments were performed on heating the sample at atmospheric pressure.



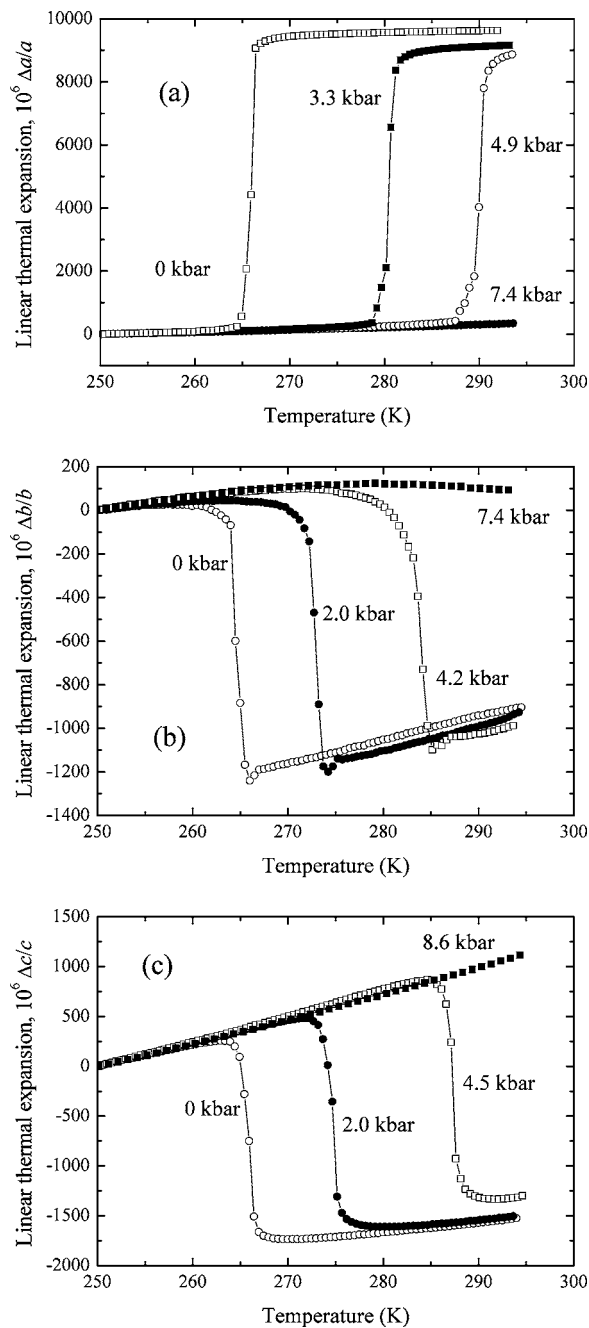


FIG. 6. LTE, defined as  $\Delta l/l = (T)/(l(250 \text{ K}) - 1)$ , as a function of the hydrostatic pressure for the three crystallographic axes: (a)  $a$ , (b)  $b$ , and (c)  $c$  axis.

magnetic and crystallographic transformations remain coupled at the studied pressure values. The difference in  $dT_C/dP$  values between polycrystalline samples ( $\sim 3 \text{ K/kbar}$ )<sup>28</sup> and the single crystals may be attributed to stress relaxation effects at the grain boundaries of the polycrystal, which may hinder the progress of the microscopic crystallographic transformations, therefore reducing the effectiveness of the applied pressure. Neither the shapes nor the sizes of the discontinuities are notably affected by pressure, suggesting that the anisotropy of the lattice parameter changes involved in the transformation is not influenced by hydrostatic pressure. It is noteworthy that a pressure of

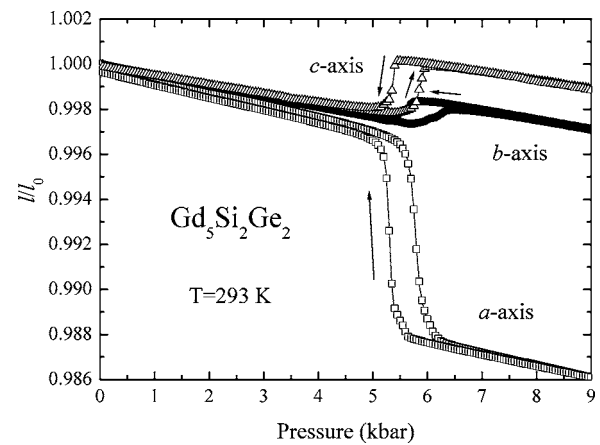


FIG. 7. Linear compressibility measured along the three crystallographic directions on increasing and decreasing pressure at  $T = 293 \text{ K}$ .

$\sim 7 \text{ kbar}$  shifts the transformation above room temperature, and consequently, anomalies at higher pressures are beyond the temperature range of our experimental apparatus. This means that the ferromagnetic  $O(I)$  state in  $\text{Gd}_5\text{Si}_2\text{Ge}_2$  exists at zero magnetic field and room temperature above  $7 \text{ kbar}$  (Fig. 6).

Compressibility measurements at room temperature along the three crystallographic axes have been performed, allowing us to demonstrate the possibility of isothermally inducing the magnetostructural transformation at zero field upon application of hydrostatic pressure. This is displayed in Fig. 7, where sharp anomalies in the volume of the sample of a size similar to those found in LTE, are observed along the three crystallographic directions at around  $6 \text{ kbar}$  during increasing pressure. The first-order character of the transformation is also confirmed, as indicated by pressure hysteresis of  $\sim 0.5 \text{ kbar}$ . The isothermal linear compressibility coefficients along the three independent axes, defined as  $\kappa_X = -(1/X)(dX/dP)_T$ , where  $X$  represents the length of the sample along  $a$ ,  $b$ , or  $c$  axes of the crystal, were calculated from the data depicted in Fig. 7 for both the low pressure  $M$ -PM and high pressure  $O(I)$ -FM phases. The obtained values are listed in Table I. We should point out the clear anisotropy found in the compressibility for the two different structures involved, which is quite reasonable taking into account the layered crystallographic structures and the directional

TABLE I. Values of the linear isothermal compressibility,  $\kappa$ , at room temperature measured along the three crystallographic axes and the total volume compressibility at the low pressure  $M$ -PM and high pressure  $O(I)$ -FM states. The percentage change of the compressibility in  $O(I)$ -FM phase relative to the  $M$ -PM phase ( $\Delta\kappa/\kappa$ ) is also provided.

	$\kappa_{M \text{ Low } P} (\text{Mbar}^{-1})$	$\kappa_{O(I) \text{ High } P} (\text{Mbar}^{-1})$	$\Delta\kappa/\kappa (\%)$
$a$ axis	0.58	0.52	-10(1)
$b$ axis	0.48	0.42	-12(1)
$c$ axis	0.42	0.37	-12(1)
$V$	1.48	1.31	-11(1)

character of the shear movement of the slabs, which is the origin of the structural transition. The values of the compressibility along the different crystallographic axes correlate reasonably well with the corresponding tendency to expand or contract in the course of the structural change. For instance, at low pressure, the largest  $\kappa$  value corresponds to the  $a$  axis,  $\kappa_a=0.58 \text{ Mbar}^{-1}$ , as expected from the tremendous elongation along the  $a$  axis through the crystallographic transformation. The  $b$  and  $c$  axes have smaller  $\kappa$  values,  $\kappa_b=0.48 \text{ Mbar}^{-1}$  and  $\kappa_c=0.42 \text{ Mbar}^{-1}$ , and they exhibit much smaller length changes than along the  $a$  axis during the structural change, see Fig. 4. This general behavior is also followed in the high pressure state, except for the values of  $\kappa$ , which are smaller in the  $O(I)$  state than in the  $M$  phase. The noted peculiarities in compressibility agree with the simple picture of a more robust crystallographic structure due to the reformation of all the covalentlike Si/Ge-Si/Ge interslab bonds in the  $O(I)$  phase. As a consequence, the value of the volumetric  $\kappa$  at high pressure is lower as well. The relative changes in the compressibilities of the two phases are the same for all the directions within the experimental resolution, as well as in the total volume change,  $\Delta\kappa/\kappa=11(1)\%$ .

#### IV. CONCLUSIONS

An investigation of the magnetic and structural properties of single crystalline  $\text{Gd}_5\text{Si}_2\text{Ge}_2$  under hydrostatic pressure has been carried out by means of magnetization, LTE, and isothermal compressibility measurements. The magneto-

structural transformation  $\text{FM-}O(I) \leftrightarrow \text{PM-}M$  with  $T_C \cong 266 \text{ K}$  is strongly dependent on pressure and  $T_C$  moves to higher temperatures at a rate of  $dT_C/dP \cong +4.8 \text{ K/kbar}$ . This rate of change is significantly larger than that determined in closely related polycrystalline samples (i.e., approximately  $+3 \text{ K/kbar}$ ). The discrepancy may be explained as a polycrystalline effect of damping the hydrostatic pressure. The reduction of the unit cell volume induced by the application of hydrostatic pressure enhances the magneto-elastic coupling in  $\text{Gd}_5\text{Si}_2\text{Ge}_2$ , extending the temperature span over which the transition takes place at any given applied magnetic field. The LTE along the three principal crystallographic axes is strongly anisotropic through the crystallographic transformation  $M \leftrightarrow O(I)$ , which coincides with the magnetic one. The dependence of the structural transition temperature on pressure agrees with that obtained from magnetic measurements. Furthermore, the size and shape of the discontinuities in strain do not change with the increasing pressure. This leads to the conclusion that the crystallographic and magnetic transformations remain coupled at all studied pressures and magnetic fields, and the anisotropic behavior of the lattice is unaffected by the hydrostatic pressure. The  $M \leftrightarrow O(I)$  transition can be also induced by isothermally applying pressure at room temperature, presenting the same features that are in the thermally induced transformation. Isothermal compressibility is anisotropic and both qualitatively and quantitatively correlates with the tendency of the lattice to expand or contract through the transition in each of the three independent crystallographic directions.

\*Author to whom correspondence should be addressed. Fax: 34-976-761229. Electronic address: morellon@posta.unizar.es

<sup>1</sup>F. Holtzberg, R. J. Gambino, and T. R. McGuire, *J. Phys. Chem. Solids* **28**, 2283 (1967).

<sup>2</sup>V. K. Pecharsky and K. A. Gschneidner, Jr., *Phys. Rev. Lett.* **78**, 4494 (1997).

<sup>3</sup>V. K. Pecharsky and K. A. Gschneidner Jr., *J. Magn. Magn. Mater.* **200**, 44 (2001).

<sup>4</sup>O. Tegus, E. Brück, K. H. J. Buschow, and F. R. de Boer, *Nature (London)* **415**, 150 (2002).

<sup>5</sup>F. Casanova, A. Labarta, X. Batlle, E. Vives, J. Marcos, L. Mañosa, and A. Planes, *Eur. Phys. J. B* **40**, 427 (2004).

<sup>6</sup>V. K. Pecharsky and K. A. Gschneidner, Jr., *J. Alloys Compd.* **260**, 98 (1997).

<sup>7</sup>W. Choe, V. K. Pecharsky, A. O. Pecharsky, K. A. Gschneidner, Jr., V. G. Young, Jr., and G. J. Miller, *Phys. Rev. Lett.* **84**, 4617 (2000).

<sup>8</sup>Q. L. Liu, G. H. Rao, H. F. Yang, and J. K. Liang, *J. Alloys Compd.* **325**, 50 (2001).

<sup>9</sup>J. Szade and G. Skorek, *J. Magn. Magn. Mater.* **196-197**, 699 (1999).

<sup>10</sup>G. Skorek, J. Deniszczyk, and J. Szade, *J. Phys.: Condens. Matter* **14**, 7273 (2002).

<sup>11</sup>B. N. Harmon and V. N. Antonov, *J. Appl. Phys.* **91**, 9815 (2002); **93**, 4678 (2003).

<sup>12</sup>G. D. Samolyuk and V. P. Antropov, *J. Appl. Phys.* **91**, 8540

(2002); V. K. Pecharsky, G. D. Samolyuk, V. P. Antropov, A. O. Pecharsky and K. A. Gschneidner, Jr., *J. Solid State Chem.* **171**, 57 (2003).

<sup>13</sup>L. Morellon, J. Blasco, P. A. Algarabel, and M. R. Ibarra, *Phys. Rev. B* **62**, 1022 (2000).

<sup>14</sup>A. O. Pecharsky, K. A. Gschneidner, Jr., V. K. Pecharsky, and C. E. Schindler, *J. Alloys Compd.* **338**, 126 (2002).

<sup>15</sup>G. H. Rao, *J. Phys.: Condens. Matter* **12** (2000) L93-L99.

<sup>16</sup>V. Hardy, S. Majumdar, S. Crowe, M. R. Lees, D. M. Paul, L. Hervé, A. Maignan, S. Hébert, C. Martin, C. Yaicle, M. Hervieu, and B. Raveau, *Phys. Rev. B* **69**, 020407(R) (2004).

<sup>17</sup>E. M. Levin, V. K. Pecharsky, and K. A. Gschneidner, Jr., *Phys. Rev. B* **62**, R14625 (2000).

<sup>18</sup>V. K. Pecharsky and K. A. Gschneidner, Jr., *Adv. Mater. (Weinheim, Ger.)* **13**, 683 (2001).

<sup>19</sup>V. K. Pecharsky, A. P. Holm, K. A. Gschneidner, Jr., and R. Rink, *Phys. Rev. Lett.* **91**, 197204 (2003).

<sup>20</sup>L. Morellon, P. A. Algarabel, M. R. Ibarra, J. Blasco, B. García-Landa, Z. Arnold, and F. Albertini, *Phys. Rev. B* **58**, R14721 (1998).

<sup>21</sup>E. M. Levin, V. K. Pecharsky, K. A. Gschneidner, Jr., and G. J. Miller, *Phys. Rev. B* **64**, 235103 (2001); E. M. Levin, K. A. Gschneidner, Jr., and V. K. Pecharsky, *ibid.* **65**, 214427 (2002); C. Magen, L. Morellon, P. A. Algarabel, and M. R. Ibarra, *J. Phys.: Condens. Matter* **15**, 2389 (2003).

<sup>22</sup>L. Morellon, J. Stankiewicz, B. García-Landa, P. A. Algarabel,

- and M. R. Ibarra, Appl. Phys. Lett. **73**, 3462 (1998); L. Morellon, P. A. Algarabel, C. Magen, and M. R. Ibarra, J. Magn. Mater. **237**, 119 (2001).
- <sup>23</sup>J. Stankiewicz, L. Morellon, P. A. Algarabel, and M. R. Ibarra, Phys. Rev. B **61**, 12651 (2000).
- <sup>24</sup>E. M. Levin, V. K. Pecharsky, and K. A. Gschneidner, Jr., Phys. Rev. B **60**, 7993 (1999); J. B. Sousa, M. E. Braga, F. C. Correia, F. Carpinteiro, L. Morellon, P. A. Algarabel and M. R. Ibarra, *ibid.* **67**, 134416 (2003).
- <sup>25</sup>L. H. Lewis, M. H. Yu, and R. J. Gambino, Appl. Phys. Lett. **83**, 515 (2003).
- <sup>26</sup>S. Fujieda, Y. Hasegawa, A. Fujita, and K. Fukamichi, J. Appl. Phys. **95**, 2429 (2004).
- <sup>27</sup>P. J. von Ranke, N. A. de Oliveira, and S. Gama, J. Magn. Mater. **277**, 78 (2004); P. J. von Ranke, N. A. de Oliveira, C. Mello, A. M. Carvalho, and S. Gama, Phys. Rev. B **71**, 054410 (2005).
- <sup>28</sup>L. Morellon, Z. Arnold, P. A. Algarabel, C. Magen, M. R. Ibarra, and Y. Skorokhod, J. Phys.: Condens. Matter **16**, 1623 (2004).
- <sup>29</sup>S. Parviainen, Phys. Status Solidi A **60**, K13 (1980).
- <sup>30</sup>L. Morellon, C. Ritter, C. Magen, P. A. Algarabel, and M. R. Ibarra, Phys. Rev. B **68**, 024417 (2003).
- <sup>31</sup>L. Morellon, Z. Arnold, C. Magen, C. Ritter, O. Prokhnenko, Y. Skorokhod, P. A. Algarabel, M. R. Ibarra, and J. Kamarad, Phys. Rev. Lett. **93**, 137201 (2004).
- <sup>32</sup>C. Magen, Z. Arnold, L. Morellon, Y. Skorokhod, P. A. Algarabel, M. R. Ibarra, and J. Kamarad, Phys. Rev. Lett. **91**, 207202 (2003).
- <sup>33</sup>M. Nazih, A. de Visser, L. Zhang, O. Tegus, and E. Brück., Solid State Commun. **126**, 255 (2003).
- <sup>34</sup>H. Tang, V. K. Pecharsky, A. O. Pecharsky, D. L. Schlagel, T. A. Lograsso, and K. A. Gschneidner, Jr., J. Appl. Phys. **93**, 8298 (2003); H. Tang, V. K. Pecharsky, G. D. Samolyuk, M. Zou, K. A. Gschneidner, Jr., V. P. Antropov, D. L. Schlagel, and T. A. Lograsso, Phys. Rev. Lett. **93**, 237203 (2004).
- <sup>35</sup>T. A. Lograsso, D. L. Schlagel, and A. O. Pecharsky, J. Alloys Compd. **393**, 141 (2004).
- <sup>36</sup>F. Casanova, A. Labarta, X. Batlle, J. Marcos, L. Mañosa, A. Planes, and S. de Brion, Phys. Rev. B **69**, 104416 (2004).
- <sup>37</sup>F. Casanova, A. Labarta, X. Batlle, J. Marcos, L. Mañosa, and A. Planes, Phys. Rev. B **66**, 212402 (2002).
- <sup>38</sup>C. A. Zimm, A. Jastrab, A. Sternberg, V. K. Pecharsky, K. A. Gschneidner, Jr., M. G. Osborne, and I. E. Anderson, Adv. Cryog. Eng. **43**, 1759 (1998).
- <sup>39</sup>Q. L. Liu, G. H. Rao, and J. K. Liang, Rigaku J. **18**, 46 (2001).
- <sup>40</sup>V. K. Pecharsky and K. A. Gschneidner, Jr. (unpublished).